Separation & Purification Reviews
Publication details, including instructions for authors and subscription information:
http://www.informaworld.com/smpp/title~content=t713597294

Separation of Latex Particles According to Size by Continuous Electrophoresis

G. D. McCann[a]; J. W. Vanderhoff[a]; A. Strickler[b]; T. I. Sacks[b]
[a] The Dow Chemical Co., Midland, Michigan [b] Beckman Instruments, Inc. Fullerton, California

To cite this Article McCann, G. D. , Vanderhoff, J. W. , Strickler, A. and Sacks, T. I.(1974) 'Separation of Latex Particles According to Size by Continuous Electrophoresis', Separation & Purification Reviews, 2: 1, 153 — 198
To link to this Article: DOI: 10.1080/03602547408068794
URL: http://dx.doi.org/10.1080/03602547408068794

SEPARATION OF LATEX PARTICLES ACCORDING TO SIZE BY CONTINUOUS ELECTROPHORESIS

G. D. McCann & J. W. Vanderhoff(1)
The Dow Chemical Co.,
Midland, Michigan 48640

and

A. Strickler & T. I. Sacks
Beckman Instruments, Inc.
Fullerton, California 92634

INTRODUCTION

When a colloidal sol is subjected to an electric field, its particles migrate toward the electrode of opposite charge. The driving force for this migration is the product of the particle charge and the electric field strength. This driving force, however, is counteracted by three retarding forces: (1) the frictional drag exerted on the particle by the medium, (2) the electrophoretic retardation produced by the flow of solvent molecules, (3) the relaxation effect introduced by the distortion of the ionic atmosphere surrounding the particle. The observed rate of migration which results from the combination of these four forces is the electrophoretic mobility.

The early investigations of electrophoretic mobility suggested that it was independent of particle size, e.g., the electrophoretic mobilities of protein molecules too small to be resolved by optical microscopy were determined by adsorbing them on the surface of microscopic-size colloidal particles and measuring the electrophoretic mobility of the protein-coated particles by the microcapillary technique(2). The values obtained agreed closely with those determined for the same protein in solution. This lack of dependence on particle size was in accord with the early theoretical work of von Smoluchowski(3) and Hückel(4), who took into account the electrophoretic retardation force, but neglected the relaxation effect. These authors found that the electrophoretic mobility is proportional to the zeta potential of the particles and the dielectric constant of the medium and inversely proportional to the viscosity of the medium. The fact that the expressions of von Smoluchowski and Hückel differed by a factor of 1.5 was resolved by Henry(5), who gave a critical analysis of their underlying assumptions. In taking into account the electrophoretic retardation force, Henry postulated that the electrophoretic mobility is also a function of the factor $\kappa\underline{a}$, where κ is the Debye-Hückel expression for the reciprocal thickness of the electric double layer and $\underline{a}$ is the particle radius. Thus, $\kappa\underline{a}$ is a measure of the ratio of the particle radius to the thickness of the double layer. Later, the relaxation effect was taken into account in the theoretical treatments of Overbeek(6, 7) and Booth(8, 9), which were extended by Wiersema et al.(10, 11). The results of the latter analysis are summarized in Figure 1, which shows the variation of electrophoretic mobility with $\kappa\underline{a}$ as a function of the zeta potential. The values of the electrophoretic mobility increase slightly with $\kappa\underline{a}$ for low values of the zeta potential; however, for high values of the zeta potential, the electrophoretic mobility decreases to a minimum at values of $\kappa\underline{a}$ = 2-5, then increases rapidly with further increase in $\kappa\underline{a}$. The greater the value of the zeta potential, the stronger the increase in electrophoretic mobility with $\kappa\underline{a}$ at values of $\kappa\underline{a}$ larger than about 5. The underlying assumptions of the Wiersema treatment are: (1) the particles are rigid spheres of uniform dielectric constant and zero electric conductivity, with a uniform surface-charge distribution; (2) the Brownian motion of the particles and the inter-

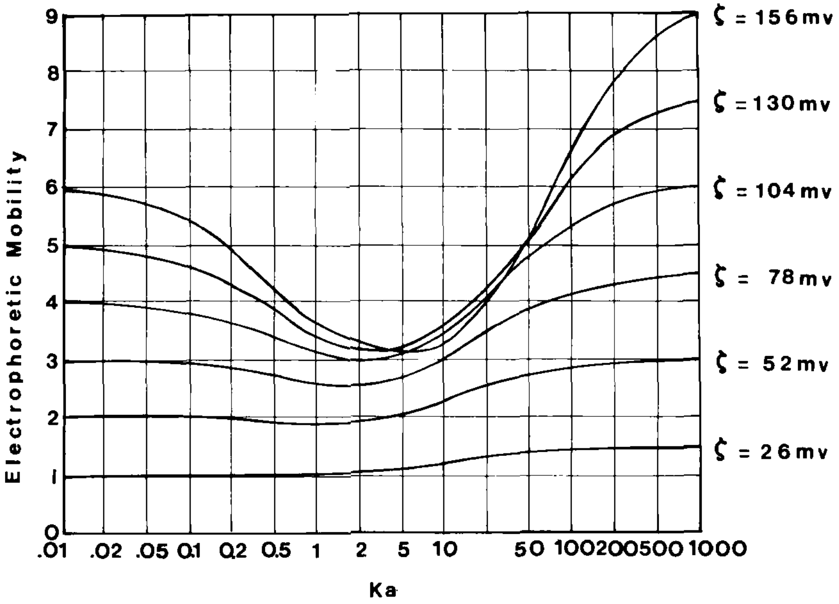

FIGURE 1

Theoretical Variation of Electrophoretic Mobility with Log Ka.(10, 11)

action between neighboring colloidal particles can be neglected; (3) the mobile part of the electric double layer is described by the classical Gouy-Chapman theory; (4) the dielectric constant and viscosity of the medium are independent of location; (5) only one type of positive and negative ions are present in the ionic atmosphere of the particle; (6) the conductance of the medium follows Ohm's law.

The strong variation of electrophoretic mobility with Ka shown in Figure 1 indicates that in principle the electrophoretic mobility can be used to determine the particle size and particle-size distribution of a colloidal sol and that electrophoresis can be used to fractionate the particles according to size. Assuming that the surface characteristics of all particles in a given sol are the same, the factor $\kappa \underline{a}$ varies only according to particle size. Thus, a sol comprised of a distribution of particle sizes should show a range of electrophoretic mobilities which corresponds to the particle-size distribution. This is the principle underlying the determination of particle size distribution by continuous particle electrophoresis. It is obvious that the method is more applicable to those sols of high zeta potential than to those of low zeta potential.

Today synthetic polymer latexes are used in many large-volume applications, e.g., paint, paper coatings, carpet backings, textile sizes, foam, and cement. The production of these latexes by the complex process of emulsion polymerization is therefore of considerable practical importance. Many applications require the close control of the latex particle size and particle-size distribution in production; however, the complexities of the emulsion polymerization process frequently make this control difficult. Therefore, it is important to develop methods to determine latex particle size and particle-size distribution. Many methods have been used, e.g., electron microscopy, light scattering, soap titration, ultracentrifugation, small-angle X-ray scattering, and flow ultramicroscopy. Of these, only electron microscopy and ultracentrifugation give direct measurements of the particle-size distribution; however, neither technique is suitable as a routine control analysis. Moreover, because of the growing use in recent years of semi-continuous or continuous emulsion polymerization processes, it is desirable to develop a method to determine the latex particle size distribution <u>rapidly</u>, so that the results obtained can be used to control the emulsion polymerization process.

Continuous particle electrophoresis offers the possibility to determine latex particle-size distributions rapidly and accurately, provided the particles possess a sufficiently-high zeta potential in a medium of suitable ionic strength. It also offers the possibility to separate latex particles (or other particles in their size range such as living cells or subcellular particles) according to size, on a preparative basis.

Separations by continuous particle electrophoresis have been accomplished by Hannig(12), who showed that, if a dispersion is introduced into a flowing stream of electrolyte and a voltage gradient is applied at right angles to this flow, the particles can be separated according to their varying surface charges. The cell was formed by two 50-cm glass plates 0.5-1.0 mm apart; its angle with the horizontal could be varied, but most experiments were carried out at 45°. Using different electrolytes, Hannig was able to separate mixtures comprised of: (1) dyestuffs; (2) amino acids; (3) peptides degraded from collagen; (4) serum proteins; (5) canine and human erythrocytes. Later, he improved his technique, mounting the cell vertically and stabilizing the voltage gradient, so that larger particles could be separated(13). His successful separations included: (1) the cell components of green spinach; (2) rat liver homogenate; (3) blood cells into erythrocytes, lymphocytes, granulocytes, and monocytes; (4) tumor cells from erythrocytes and unaltered leucocytes. Strickler et al.(14, 15) used a rectangular cell with a vertically-flowing electrolyte curtain (2.5 cm wide, 18-45 cm long, 1.5 mm thick), which featured rapid electrolyte curtain flow and rapid particle separation. They clarified the effect of the cell-wall zeta potential on resolution and the importance of confining the particles to the center of the 1.5 mm-thick curtain. Their separations included mixtures of E. coli bacteria with such inorganic pigments as Prussian Blue and Ultramarine Blue.

The purpose of this paper is to describe the instrument developed for continuous particle electrophoresis and its application to the determination of latex particle-size distributions. Included is the separation of latexes according to particle size, the factors which affect this separation, the experimental difficulties involved, and the correlation between the experimental results and the theory of electrophoresis.

APPARATUS

Figure 2 shows a schematic diagram of the Beckman Continuous Particle Electrophoresis apparatus. The electrophoresis cell defines a curtain-flow space 1.5 mm thick, 5.0 cm wide, and 50 cm long. Of the 50 cm-length, only 30 cm are subjected to the electric field. The electrolyte solution is fed by gravity into the top of the cell from a constant-level source. At the bottom of the cell, the electrolyte curtain empties through a set of 48 0.25 mm-I. D. tubes spaced with their centers 1 mm apart, so that it is separated into 48 fractions of equal volume. The electrodes are separated from the electrolyte curtain by membranes, each of which forms a wall in a compartment through which is pumped another supply of the same electrolyte solution. The colloidal sol is injected near the top-center of the flowing electrolyte curtain. At zero voltage gradient, the particles of the sol descend vertically in a fine stream, 0.15-0.25 mm in diameter. When the voltage gradient is applied, this stream is split into components descending at slightly different angles, the resultant of the vertical velocity (the same for all particles) and the lateral velocity (dependent on the electrophoretic mobilities of the particles and the field strength). Thus, the sample stream is spread out between the electrodes, according to the electrophoretic mobilities of the particles. It then flows past a millimeter scale, which is illuminated (dark-field) and read under low magnification, so that the lateral displacement of the stream can be measured. At the bottom of the cell, the sample stream is carried out by the electrolyte curtain into the 48 collecting tubes, to give fractions which can be characterized later. Convective disturbance of the particle streams due to ohmic heating of the electrolyte curtain is minimized by circulating low-tempera-

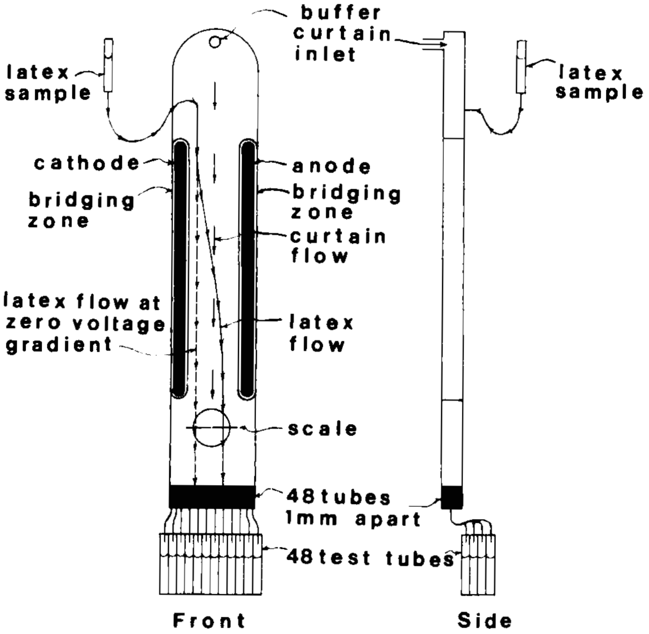

FIGURE 2

Schematic Diagram of the Continuous Particle Electrophoresis Instrument.

ture water through the faceplate of the cell. The instrument can accommodate any particle size up to 100μ diameter.

Figure 3 shows a flow diagram of the auxiliary equipment. The electrolyte solution is fed by gravity through a flow meter to the electrophoresis cell. The electrolyte solution in the reservoir is maintained at a constant level by a peristaltic pump. This pumps electrolyte solution from storage through a filter to the constant-level overflow bottle. A separate electrolyte solution reservoir serves for the electrode-rinsing operation. A centrifugal pump transfers electrolyte solution from this reservoir to a pressure bottle, which in turn feeds the solution to the bottom of the two

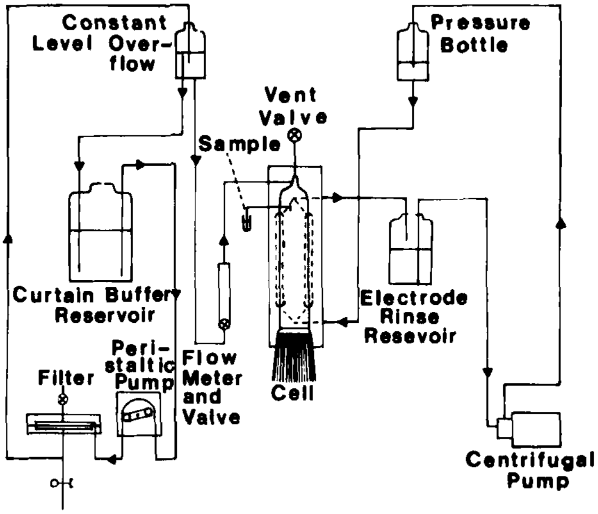

FIGURE 3

Schematic Diagram for the Auxiliary Equipment for Continuous Particle Electrophoresis.

electrode chambers. The effluent from both chambers is mixed and returned to the rinse-electrolyte reservoir.

The sample-feed system is designed to give a constant rate of flow of the colloidal sol. Water is electrolyzed in a small vessel to give hydrogen and oxygen, which are then fed into the sample container so that the pressure of this gas forces the sample through a thin tube into the cell. The use of an adjustable current for electrolysis allows an accurate control of the sample flow rate with a convenient meter readout.

As mentioned earlier, the separated particle streams flow past a mm scale in the cell window, which can be used to measure their lateral displacement. To characterize a separation, however, it is important not only to measure the lateral displacement, but also to visualize the cross-section of the particle stream. This is accomplished with the cross-section illuminator (CSI) shown schematically in Figure 4 which comprises a light bulb with a straight-line incandescent filament mounted horizontally parallel to the cell walls behind the cell window and a lens stopped down with a horizontal slit to image this source in the plane of the electrolyte curtain. Thus, a thin, horizontal blade of light sections the electrolyte curtain, making the cross-sections of the particle streams visible from the front of the cell.

The separation of the particles can be characterized in four ways: (1) by visual readings of the lateral displacement using the mm scale; (2) by characterizing the collected fractions by some technique such as electron microscopy or light scattering; (3) by photographing the separated particle streams and analyzing the photograph with a densitometer; (4) by measuring the variation of scattered-light intensity with lateral displacement.

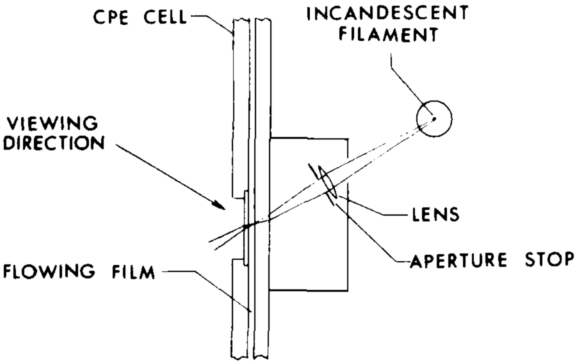

FIGURE 4

Schematic Diagram of the Cross-Section Illuminator.

For the first method, one need only make the required measurements of lateral displacement using the mm scale (see Figure 5); however, this method is applicable only to those samples which form one or more narrow streams upon electrophoresis, i. e., those which have narrow distributions of electrophoretic mobilities.

For the second method, the instrument is operated for a sufficient period of time so as to give fractions large enough to be characterized. Electron microscopy of these fractions not only allows a visualization of

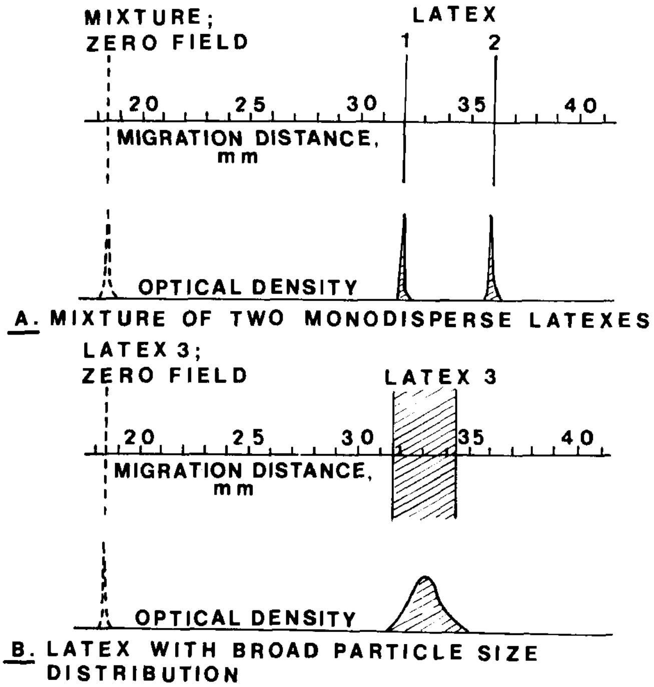

FIGURE 5

Schematic Depiction of the Separation of a Mixture of Two Monodisperse Latexes and a Latex of Broad Particle Size Distribution.

the discrimination of separation, but it also requires only a very small sample, e.g., one drop containing 10 ppm particles. The fractions can also be characterized by light scattering, but the concentration of particles must be known to give an accurate measure of particle size. Both electron microscopy and light scattering are complicated by the presence in the fractions of the curtain electrolyte, the concentration of which may be appreciable compared to that of the particles. The electrolyte concentration may be reduced before examination by dialysis or ion exchange. In the case of electron microscopy, the electrolyte may be removed by washing the dried specimen. All these techniques, however, involve extra steps; moreover, they must be used with care, to avoid altering the size distribution of the fractions.

For the third method, the separated streams of particles are photographed, and the photograph is analyzed with a densitometer. To do this, the surface of the faceplate and rearplate of the cell must be free from even minute scratches because the back-illumination of the separated streams (i.e., by the light source mounted inside the instrument) causes any scratches or imperfections in the surfaces of the cell through which the light passes to give glare. The human eye perceives but disregards these extraneous sources of light, but the densitometer is less discriminating.

The fourth method is to measure the variation of scattered light intensity with lateral displacement. Several instruments have been developed to do this. Each gave better results than its predecessor; however, the definitive instrument has not yet been developed. Nevertheless, the most recently developed instrument gives results which are good enough to verify the discrimination of the separation technique (Figure 6). The optical layout of these instruments differed somewhat, but the general principle was the same, i.e., the particle streams were illuminated by a light source mounted at an angle of 45-90° to the vertical plane of the cell midpoint, and

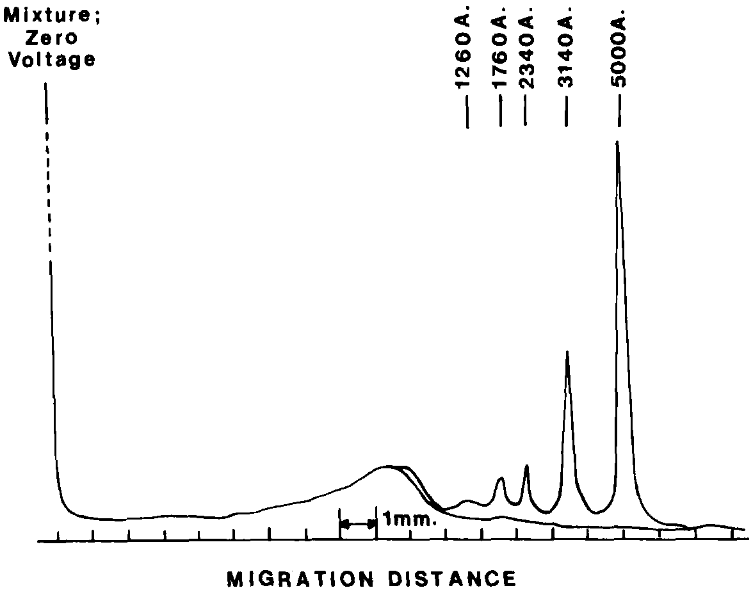

FIGURE 6

Variation of Scattered-Light Intensity with Migration Distance as Determined by a Photometric Scanner.

the light transmitted or scattered at 90° to the incident beam was measured by a photoelectric cell. The photoelectric cell was mounted on a motor-driven rack, so that it could traverse the field laterally at constant speed. The output from the photoelectric cell was picked up as a recorder trace, to give a measure of the variation of scattered-light intensity with lateral displacement. Figure 6 shows such a recorder trace for a mixture of five monodisperse latexes.

To obtain quantitative results with the latter two methods, the scattered-light intensity at a given lateral displacement, corresponding to particles of a given size, should be proportional to the particle concentration. However, the scattered-light intensity at a given wavelength and concentration of dispersed phase is not a monotonic function of particle size. Therefore, a weighting function must be applied to the recorder trace of the scattered-light intensity-displacement curve to transform it to a particle-size distribution curve. The mathematical form of this weighting function is complex because the particle-size range spans that of both Rayleigh and Mie scattering and, therefore, it has not been derived. Instead, as will be seen later, the scattered-light intensity can be calibrated with known concentrations of different-size monodisperse latex particles.

To minimize the broadening of the particle streams by electro-osmotic flow, the zeta potentials of the faceplate and rearplate of the electrophoresis cell which contact the flowing curtain should be as similar as possible and of an appropriate value relative to the average zeta potential of the particles. Ideally, the zeta potential of the walls should be such that the electro-osmotic velocity of the liquid adjacent to the walls is equal and opposite to the average electrophoretic velocity of the particles (with respect to the medium). Since the faceplate is glass and the rearplate is Plexiglas, the cell-wall zeta potentials may be quite different, although this difference is usually reduced gradually by the adsorption of sample components onto the walls. The desired cell-wall zeta potentials have been achieved by two treatments: (1) Dow Corning 1201 Silicone primer is applied to the faceplate and dried, then Dow Corning Hi-Vac Silicone grease is applied as a top coat; the same grease is applied directly without the primer to the rearplate; (2) the silicone primer is applied to the faceplate and dried, then the surface is covered with a sheet of pressure-sensitive 3M Polyester Film Tape No. 850, over which is brushed a thin film of collodion (Baker U. S. P.) thinned with an equal volume of methyl cellosolve; the collodion-coated polyester film is applied to the rearplate without the primer, or the collodion solution is applied directly to the Plexiglas surface. Both of these treatments last for weeks or months of continual use.

LATEX SAMPLES

Most of the experiments described herein used monodisperse polystyrene latexes prepared by either conventional batch-type emulsion polymerizations or seeded emulsion polymerizations, in which a previously-prepared latex is grown to a larger particle size by adding more monomer and initiator(16). These preparations used plant-grade inhibitor-free styrene monomer, deionized water, technical-grade emulsifiers, and reagent-grade sodium bicarbonate buffer and potassium persulfate initiator. The particle diameters of the latexes were determined by electron microscopy using the method described previously(17). The polymerization is initiated by sulfate ion-radicals formed by the decomposition of aqueous persulfate ion. This mechanism incorporates sulfate endgroups into the polymer molecules, some of which remain on the particle surface. Therefore, the latex particles are stabilized by two types of anionic groups: (1) adsorbed polymerization emulsifier; (2) sulfate endgroups of the polymer chains which remain on the particle surface. Moreover, the aqueous phase of the latexes contains a certain amount of electrolyte, i. e., the decomposition products of the persulfate and the buffer used to keep the pH at the desired level.

The latexes were treated in three different ways before being subjected to continuous particle electrophoresis: (1) they were used "as is," i. e., still containing the emulsifier and electrolyte from the polymerization reaction; (2) the adsorbed emulsifier and solute electrolyte were removed quantitatively by ion exchange, so that the particles were stabilized only by the residual sulfate endgroups (H^+ form) at the particle surface; (3) the ion-exchanged samples were stabilized further by the addition of emulsifier. The ion exchange was carried out using the technique described previously(18-21). The purpose of removing the adsorbed emulsifier and solute electrolyte, leaving the particles stabilized only by the sulfate endgroups, is to prepare a model colloid, i. e., uniform spheres with a constant and known surface charge density. The number of the residual sulfate endgroups (H^+ form) was determined by conductometric titration with sodium hydroxide; this value, along with the surface area determined by electron microscopy, can be used to calculate the surface charge density. These parameters were determined for a series of monodisperse polystyrene latexes which were used as model colloids in investigations of viscosity, conductance, stability, adsorption, interference colors, and ultracentrifugation(19, 22). Further work showed that there are also nonionic hydroxyl groups on the particle surface in some latexes(23). Table I gives the particle sizes and surface charge densities (for the ion-exchanged form) of the latexes used in this study. Other latexes used are described in the following sections.

The microcapillary electrophoretic mobility measurements were carried out in the Zeta-Meter microcapillary cell. Other experiments carried out are described in the following sections.

EXPERIMENTAL TECHNIQUES AND RESULTS

The latex samples were diluted to about 0.1% solids for examination. The diluted latex was placed in the sample container and the electrolyte curtain flow was started. When the electrolyte curtain and electrode-rinse flow rates became constant, the capillary stream was allowed to descend vertically at zero voltage gradient for a short time, to make sure that the system was performing in a stable manner. Then the voltage gradient was

TABLE I

Monodisperse Polystyrene Latexes

Latex	Ave. Particle Diam., A.	Std. Dev. A.	# of Meas.	Surf. Chge. Density (18-21), μC/cm^2
A	440	79	---	---
B	910	58	206	4.7
C	1090	26	318	2.1, 2.5
D	1260	43	328	1.7
E	1760	23	279	1.7, 1.6
F	2340	26	245	2.0
G	2480	41	31	5.7
H	3120	22	185	2.2
I	4470	104	35	8.1
J	5000	27	130	2.4, 2.1
K	7140	53	142	---
L	7950	44	136	0
M	10400	71	36	7.4, 5.8
N	10990	59	106	5.7
O	13050	158	142	4.6
P*	18600	70	56	---
Q*	19470	77	154	---
R	20200	135	54	3.8

* - polyvinyltoluene

applied, and the latex stream moved laterally according to the electrophoretic mobilities of the particles. The equilibration of the particle stream takes place within the time required for transit of the curtain, i. e., in less than one minute, but the equilibration of the cell walls to a steady-state temperature takes a little longer; the latter equilibration shifts the position of the particle stream slightly. After equilibration, the separation is characterized using one of the methods described above.

The first experiments involved the separation of mixtures of two monodisperse latexes. This is depicted schematically in Figure 5: upon electrophoresis, the particle stream splits into two narrow streams separated by a region which contains no particles. Three mixtures prepared using Latexes F, J, N, and P contained the following particle sizes: 0.23 and 0.50μ; 0.50 and 1.10μ; 0.50 and 1.86μ. A few drops of the latex mixture were added to the 1×10^{-3} M Beckman B-2 Veronal or sodium barbital buffer (diethyl barbituric acid/sodium diethyl barbiturate; pH 8.6) used as the electrolyte curtain. The temperature of the cooling water in the faceplate was 10° C, the electrolyte curtain flow rate 20 ml/min., the voltage gradient 100 volts/cm. All three mixtures separated into two narrow fractions, and the major part of each fraction was found in a single collecting tube. The fractionation was continued until all of the mixture was delivered through the instrument. The fractions were then centrifuged to concentrate the latex particles, two-thirds of the supernatant layer was decanted and replaced with water, and the particles were resuspended. Examination of the six fractions by electron microscopy showed that the separations were virtually perfect for all three mixtures. In each fraction, several electron microscope fields had to be examined before a single off-size particle could be seen. Thus, these experiments demonstrated that it is possible to separate mixtures of monodisperse latexes almost quantitatively and that this separation can form the basis for a determination of particle size and particle-size distribution.

There are three important parameters in the operation of the continuous particle electrophoresis cell: (1) the curtain electrolyte flow rate $\underline{F}$; (2) the voltage gradient $\underline{E}$; (3) the ionic strength of the medium $\underline{I}$. The relationship between the migration distance $\underline{D}$ (i. e., the lateral displacement in mm) of the particles and the parameters $\underline{F}$ and $\underline{E}$ is of the form

$$D = KE/F \tag{1}$$

where $\underline{K}$ is a constant. The effect of ionic strength is more complex and depends upon the values of $\kappa \underline{a}$, which may range from 0.01 to 300. For values of $\kappa \underline{a}$ greater than about 300, the relationship becomes

$$D = K_1 \zeta E/FI^{\frac{1}{2}} \qquad (2)$$

where ζ is the zeta potential of the particles and K_1 is a constant.

Preliminary experiments were carried out to determine the variation of D with E, F, and I. Tables II, III, and IV give the calculated values of D/E, DF, and $DI^{\frac{1}{2}}$, respectively. These quantities should be constant for a given latex, independent of voltage gradient, electrolyte curtain flow rate, and electrolyte concentration, respectively, if equation (2) holds. It can be seen that the values of D/E are approximately constant for a given latex and independent of E, thus confirming the proportionality between migration distance and voltage gradient. Also, the values of DF are approximately constant and independent of F, thus confirming the inverse proportionality between migration distance and electrolyte curtain flow rate. However, the values of $DI^{\frac{1}{2}}$ actually increase slightly with increasing ionic strength, thus indicating that the migration distance does not vary in proportion to the reciprocal square root of the ionic strength as predicted by equation (2) (however, equation (2) is valid only for $\kappa a > 300$, a range considerably above that applicable to latex particles, as will be seen later).

In other experiments, the effect of latex treatment was investigated. Table V summarizes the results obtained using the latexes "as is," after ion exchange, and after ion exchange-plus-additional-emulsifier. It can be seen that the removal of adsorbed emulsifier by ion exchange does not affect the migration distance appreciably. Also, the addition of Aerosol MA emulsifier (American Cyanamid Co.) to the ion-exchanged latex does not change the migration distance appreciably, but does broaden the particle stream; in this broadening, the trailing edge of the stream is spread out rather than the leading edge. Table V also shows that the measurements at different voltage gradients give consistent results, both with respect to variation of voltage gradient and treatment of the latex before examination.

TABLE II

Effect of Voltage Gradient on Migration Distance

10°C. ; sodium barbital electrolyte

Particle Diameter, A.	Voltage Gradient, volts/cm	Migration Distance, mm	D/E, cm^2/volt, x 10^2
2480*	50	9.0-9.5	1.80-1.90
	70	12.0-13.0	1.71-1.86
	90	14.5-16.0	1.61-1.78
4470*	50	10.8	2.16
	70	14.5-15.0	2.07-2.14
	90	18.5-19.0	2.06-2.11
5000*	50	11.2	2.24
	70	16.2-16.7	2.31-2.39
	90	20.2-20.7	2.24-2.30
10400*	50	14.3	2.86
	70	18.5-19.0	2.64-2.71
2480**	50	7.0-8.5	1.40-1.70
	70	12.0-12.5	1.71-1.79
5000**	50	11.5	2.30
	70	15.5	2.21
10400**	50	12.5-13.0	2.50-2.60
	70	17.5-19.5	2.50-2.79
2480***	50	9.0-9.5	1.80-1.90
	70	13.0-13.5	1.86-1.93
5000***	50	11.0-12.0	2.20-2.40
	70	15.5-17.5	2.21-2.50
10400***	50	13.0-14.5	2.60-2.90
	70	18.0-20.5	2.57-2.93

* - electrolyte curtain flow rate 16.5 ml/min; 1×10^{-3} M electrolyte
** - electrolyte curtain flow rate 18.0 ml/min; 1×10^{-3} M electrolyte
*** - electrolyte curtain flow rate 18.0 ml/min; 2×10^{-3} M electrolyte

TABLE III

Effect of Electrolyte Curtain Flow Rate on Migration Distance

10°C; 70 volts/cm; 1×10^{-3} M sodium barbital electrolyte

Particle Diameter, A.	Flow Rate ml/min	Migration Distance, mm	DF, cm ml/min
2480	15.0	13.5-15.0	20.3-22.5
	16.5	12.0-13.0	19.8-21.5
	18.0	12.0-12.5	21.6-22.5
5000	16.5	16.0-16.5	26.4-27.2
	18.0	15.5	27.9
10400	15.0	19.5-20.0	29.3-30.0
	16.5	18.5-19.0	30.5-31.4
	18.0	17.5-19.5	31.5-35.1

TABLE IV

Effect of Ionic Strength on Migration Distance

10°C. ; 18.0 ml/min; sodium barbital electrolyte

Particle Diameter, A.	Electrolyte Concn., M	Migration Distance, mm	$D (I)^{\frac{1}{2}}$, cm, $\times 10^2$
2480*	1×10^{-3}	7.0-8.5	2.21-2.69
	2×10^{-3}	9.0-9.5	4.02-4.25
5000*	1×10^{-3}	11.5	3.63
	2×10^{-3}	11.0-12.0	4.92-5.36
10400*	1×10^{-3}	12.5-13.0	3.95-4.11
	2×10^{-3}	13.0-14.5	5.81-6.48
2480**	1×10^{-3}	12.0-12.5	3.79-3.95
	2×10^{-3}	13.0-13.5	5.81-6.03
5000**	1×10^{-3}	15.5	4.90
	2×10^{-3}	15.5-17.5	6.93-7.82
10400**	1×10^{-3}	17.5-19.5	5.53-6.16
	2×10^{-3}	18.0-20.5	8.05-9.16

* - voltage gradient 50 volts/cm

** - voltage gradient 70 volts/cm

TABLE V

Effect of Ion Exchange and Emulsifier Addition on Migration Distance

10°C.; 16.5 ml/min; 1×10^{-3} M sodium barbital electrolyte

Particle Diameter, A.	Migration Distance at Specified Voltage Gradients, mm		
	50 volts/cm	70 volts/cm	90 volts/cm
2480	9.0-9.5	12.0-13.0	14.5-16.0
2480*	8.7-9.2	12.2-13.2	14.7-16.2
2480**	6.5-10.5	9.5-11.8	13.0-18.5
4470	10.8	14.5-15.0	18.5-19.0
4470*	11.0	15.0	19.0-19.8
4470**	7.5-11.5	11.5-15.5	16.5-19.5
5000	11.2	16.2-16.7	20.2-20.7
5000*	12.3	16.8	20.5-21.0
5000**	10.7-13.2	8.7-17.7	11.2-22.2
10400	14.3	18.5-19.0	---
10400*	13.4-14.5	18.5-19.0	---
10400**	13.2-14.2	18.2-21.2	---

* - latex ion-exchanged to remove emulsifier and electrolyte

** - Aerosol MA solution added to ion-exchanged latex

The separation of mixtures of monodisperse latexes has been demonstrated so effectively that it has been used to assess the resolution capability of the instrument. For example, a mixture comprised of 1260 and 1760 A. diameters (Latexes D and E) was separated into two discrete 0.1 mm-width streams about 1 mm apart. No evidence of latex particles was seen in the intervening distance between the two streams. In another example, a mixture comprised of 440 and 1090 A. diameters (Latexes A and C) were separated into 0.1 mm-width streams about 1 mm apart. These separations were followed not only by visual readings of the migrations distances, but also by the variation of scattered-light intensity with migration distance. Figure 6 shows a recorder trace depicting the separation of a mixture of five different particle sizes. Five distinct peaks can be seen, each corresponding to one of the latexes in the mixture; however, the failure of the signal to return to the base line between the particle streams is not in accord with visual observations, which indicates that there are no particles between the separated streams. In other experiments, mixtures containing as many as 10 different sizes ranging from about 0.1μ to about 2μ were separated into narrow streams, each stream corresponding to a given latex and all separated from one another by regions which contain no particles. Such discrimination offers the promise that samples with a broad distribution of particle sizes can be determined with accuracy and precision, as depicted schematically in Figure 5.

Figure 7 shows the variation of migration distance with particle diameter for three electrolyte concentrations: 1×10^{-3} M sodium lauryl sulfate; 2.5×10^{-3} and 5×10^{-4} M sodium barbital. It is obvious that the variation in migration distance is great enough to obtain a total separation since each particle stream is only about 0.1 mm in width and there is no evidence of latex particles in the intervening regions. For the two series in sodium barbital, the variation of migration distance with particle diameter at the smaller particle sizes is greater at 2.5×10^{-3} M than at 5×10^{-4} M concentration, indicating that the sensitivity of the technique can be altered somewhat to emphasize the separation of the smaller or larger particles. The two series in 1×10^{-3} M sodium lauryl sulfate gave slightly different, but internally consistent, curves. Note that the values for Latex L (7950 A.) fell below the curves in both series; this anomalously small migration distance is to be expected because of its experimentally-determined zero surface charge density (Table I).

Generally, in a given series of monodisperse latexes, the migration distance increased with increasing particle size. This increase is consistent with the theoretical curves of Figure 1 which show a strong increase in the electrophoretic mobility with log $\kappa \underline{a}$ at high values of the zeta potential.

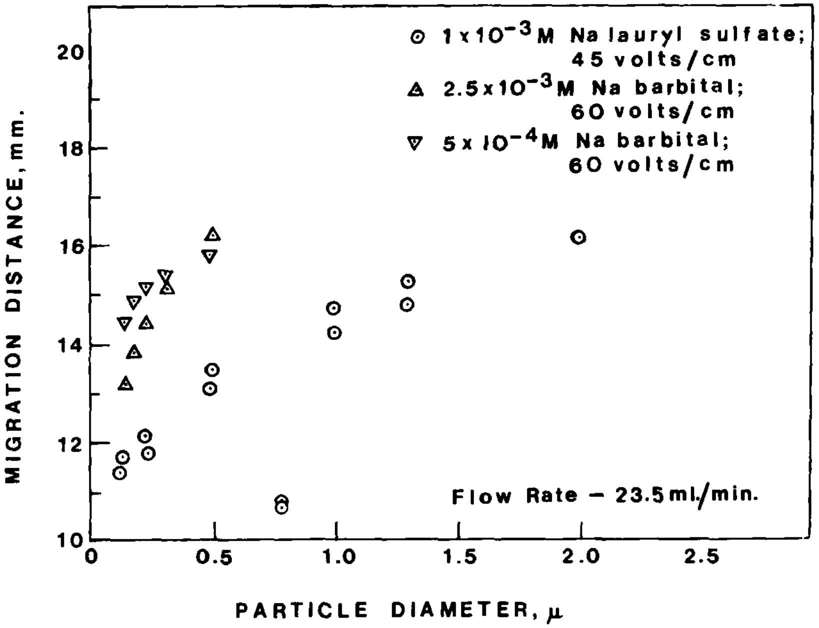

FIGURE 7

Variation of Migration Distance with Particle Diameter for Monodisperse Polystyrene Latexes.

However, the same curves also show a minimum in electrophoretic mobility in the range of $\kappa\underline{a}$ = 2-5 and negative slopes at lower $\kappa\underline{a}$ values, indicating that under certain conditions a reversal in the order of electrophoretic mobility with respect to particle size should be observed. This has been confirmed experimentally with particles of 440 and 910 A. diameter (Latexes A and C), which were run both separately and in mixture, using a voltage gradient of 110 volts/cm and an electrolyte curtain flow rate of 11.0 ml/min. The separated streams were identifiable by the much lower scattering power of the 440 A.-diameter particles. In 1×10^{-3} M sodium barbital, the two different sizes fell in the normal order, the migration distance of the larger size being slightly greater than that of the smaller size. However, in 3.5×10^{-4} M sodium barbital, the migration distances were 33.3 and 33.1 mm for the 440 A. and 910 A.-diameter sizes, respectively. Thus, at a sufficiently-low electrolyte concentration, the migration distance of the smaller particles was actually slightly greater than that of the larger particles.

In the foregoing sections, the migration distances used to characterize the particle separations were expressed as a single value (or a narrow range of values) read from the mm scale in the cell window; however, the cross-section of the particle stream, as viewed with the cross-section illuminator (Figure 4), is also an important parameter of the particle separation. The visualization of the cross-section of the particle stream permits: (1) a judgment as to whether the cell-wall zeta potential is suitable for good resolution and, if not, in which direction it should be changed by the appropriate coating; (2) a more accurate interpretation of the scattered -light intensity-migration distance curves by determining whether it is the leading or trailing edge of the stream that indicates the electrophoretic mobility; (3) the use of the photographic techniques described below to determine relative values of the electrophoretic mobility with higher precision.

The cross-section of a stream of monodisperse particles is generally crescent-shaped. This shape results from the fact that particles which descend at different depths within the curtain are subjected not only to different vertical liquid velocities but also to different lateral liquid velocities due to the electro-osmotic effect. For a stream of electrophoretically homogeneous particles at a fixed lateral position in the electrolyte curtain, but distributed over a range of depths in the curtain thickness, the lateral displacement $\underline{D}$ is given as a function of depth-position by

$$D = (H/y'_0)\ [(u+u_{LW})/(1-z^2) - (3/2)u_{LW}] \qquad (3)$$

where $\underline{z}$ is a measure of the depth in the cell defined as 0 at mid-depth and ± 1 at the front or rear walls, respectively, $\underline{H}$ the height of the electric field zone, $\underline{y'_0}$ the vertical liquid velocity at mid-depth, $\underline{u}$ the lateral particle velocity relative to the liquid (proportional to the electrophoretic mobility), and $\underline{u}_{LW}$ the lateral electro-osmotic velocity of the liquid adjacent to the cell wall. The velocity $\underline{u}_{LW}$ is proportional to the cell-wall zeta potential in accord with the Helmholz-Smoluchowski equation.(24) The velocities $\underline{u}$ and $\underline{u}_{LW}$ are defined as positive when the particle or boundary liquid movement is directed toward the anode. If both the walls and the particles are negatively-charged, $\underline{u}$ is positive and $\underline{u}_{LW}$ negative. Figure 8 shows a family of crescent-shaped cross-sections observed with a mixture of monodisperse polystyrene latexes (each having a different $\underline{u}$ value). In this figure, the anode is at the right and the particle streams are numbered from the left; for streams 1-3, $(\underline{u}+\underline{u}_{LW})$ is negative; for stream 4, $\underline{u}=-\underline{u}_{LW}$, giving maximum resolution in this portion of the pattern; for streams 5 and 6, $(\underline{u}+\underline{u}_{LW})$ is positive. When the crescents are convex toward the anode (streams 1-3), the resolution can be increased by making the cell-wall zeta potential less negative; for bands of the reverse curvature, the cell-wall zeta potential should be shifted in the opposite direction.

Since the exact value of the cell-wall zeta potential is not critical for most work, only a few alternate coatings are needed to adjust it to a satisfactory range. In the electrolyte solutions used here, uncoated Mylar polyester films were found to have a relatively-high zeta potential, collodion an intermediate zeta potential, and gelatin (applied over a Mylar substrate) a low zeta potential.

The resolution is also improved by reducing the sample flow-rate, which reduces the $\underline{z}$ range. When the sample flow-rate is increased such that $\underline{z}$ approaches ± 1, the arms of the crescent extend asymptotically toward the walls; however, the apex of the crescent $(\underline{z}=0)$ remains fixed.

If the lateral displacement $\underline{D}_r$ at which curvature reversal occurs is known, the cell-wall zeta potential ζ_w and the electro-osmotic component $\underline{D}_{eo}$ of the particle displacement observed at the mid-plane ($\underline{z}$ = 0) can be estimated. The value of $\underline{D}_r$ is estimated by using a series of monodisperse polystyrene latexes of different particle sizes (Figure 8). Since $\underline{D}_{eo}$ is the same as the deflection observed with a zero-mobility band (u = 0), equation (3) gives at $\underline{z}$ = 0

$$D_{eo} = u_{LW}\ H/2y_o' \qquad (4)$$

whereas at the reversal point, i.e., where $\underline{u} = -\underline{u}_{LW}$,

$$D_r = -3u_{LW}H/2y_o' \qquad (5)$$

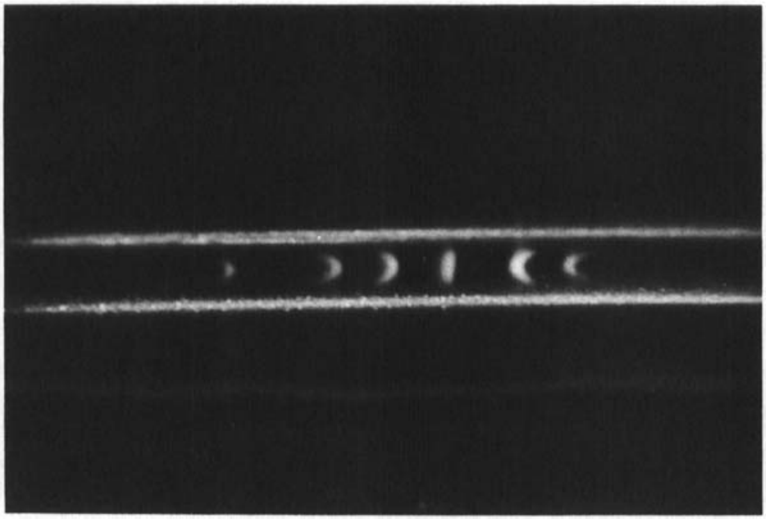

FIGURE 8

Photograph of Crescent-Shaped and Elliptical Cross-Section of Separated Streams of Monodisperse Polystyrene Latexes.

Therefore,

$$D_{eo} = D_r/3 \tag{6}$$

From the known profile of the lateral (electro-osmotic) liquid velocity,

$$u_{LW} = -2u_{LM} \tag{7}$$

where u_{LM} is the *mid-plane* electro-osmotic velocity. Since u_{LM} is given by D_{eo} divided by the transit time at mid-depth in the medium,

$$u_{LW} = 2X_{eo}y'_o/H \tag{8}$$

or

$$u_{LW} = -(2/3)X_r y'_o/H$$

From the Helmholz-Smoluchowski(24), this now yields the cell-wall zeta potential

$$\zeta_W = 4\pi\eta u_{LW}/E\epsilon \tag{9}$$

where η and ϵ are the viscosity and the dielectric constant of the medium, respectively. Alternatively, a zero-mobility sample can be used to determine D_{eo} directly, and u_{LW} as well as ζ_W can be derived from equations (8) and (9), but such particles which scatter light and yet have zero mobility in various media are not readily available (however, see Latex L in Table I).

The combination of the cross-section illuminator with continuous particle electrophoresis gives an unusually precise method for the determination of *relative* electrophoretic mobilities. Two monodisperse polystyrene latexes of about 0.1μ and 1.0μ particle diameter are used as *internal* standards, admixed with the latex sample to be determined. The photograph of the particle stream cross-sections (Figure 8) shows the cell-walls as two parallel lines due to the light-scattering properties of a coating applied to the cell wall at the window. The positions of the sample particle streams are measured on a scale which assigns values of zero and unity to the streams of the smaller and larger reference particles, respectively. The position of the streams is determined at a depth $\underline{z} = 0$, i. e., at the intersection of the crescents with a parallel line drawn half-way between the two wall lines.

This method has the important advantage that the relative mobility values thus derived are independent of fluctuations in the field strength, electrolyte curtain flow rate, or magnitude of the electro-osmotic component. This is shown by the fact that the observed displacement $\underline{D}$ (in the mid-plane of the curtain) from the zero-field position is

$$D = (KE/F)\ (\mu + \mu_{LO}) \tag{10}$$

where $\underline{\mu}$ is the electrophoretic mobility and $\underline{\mu}_{LO}$ is the electro-osmotic "mobility" of the liquid at the mid-plane ($\underline{\mu}_{LO} = -\underline{\mu}_{LW}/2$, where $\underline{\mu}_{LW}$ is the electro-osmotic "mobility" of the liquid layer adjacent to the wall). The difference between the displacements of the two reference sizes is

$$D_2 - D_1 = (KE/F)\ (\mu_2 - \mu_1) \tag{11}$$

The relative mobility RM of an unknown sample is then given by

$$RM = (D_s - D_1)/(D_2 - D_1) = (\mu_s - \mu_1)/(\mu_2 - \mu_1) \tag{12}$$

where $\underline{D}_s$ and $\underline{\mu}_s$ are the displacement and the mobility of the unknown sample, respectively. The RM values of different-size latex particles determined on different days by this technique were found to be very reproducible (standard deviation = 0.005 RM units); however, the RM values determined in one medium generally will not be applicable to another medium. If the absolute mobilities of the reference particles are determined in the same medium by an independent technique, e.g., microcapillary electrophoresis, the RM values may be converted to absolute mobilities by the relationship

$$\mu_s = RM(\mu_2 - \mu_1) + \mu_1 \tag{13}$$

In Figure 8, which shows a six component-band cross-section, the crescents occupy a greater thickness of the curtain than is normal under these conditions. In this case, the crescent-effect was enhanced deliberately by flattening the injection tip to a fish-tail cross-section. The sample then entered as a ribbon normal to the cell surfaces rather than as a cylinder. Similar samples using the normal injection cross-section show smaller crescents under the same conditions.

Latexes other than polystyrene can also be separated by continuous particle electrophoresis. The types investigated thus far include styrene-butadiene, vinylidene chloride, vinyl chloride, and vinyl acetate copolymers. When the migration distances of these various copolymer latexes were compared to a calibration curve determined for different-size monodisperse polystyrene latexes, the values for some samples fell above the curve, but those for most samples fell below the curve. Several samples showed very small migration distances, comparable to that of the anomalous polystyrene Latex L. This latex in microcapillary electrophoresis showed an electrophoretic mobility of essentially zero, thus confirming by independent measurements the validity of the continuous particle electrophoresis results.

Since the monodisperse polystyrene particles have a very narrow particle size distribution, the separated particle streams observed in the cell window are frequently of various colors and display higher-order Tyndall spectra. These colors are a function of the particle size and refractive index of the latex particles, and the angle between the direction of illumination and of viewing(25-27).

DISCUSSION

The migration distances of monodisperse polystyrene latexes in continuous particle electrophoresis are in qualitative accord with the Wiersema theory with respect to: (1) the variation of electrophoretic mobility with particle size; (2) the effect of ionic strength on the form of the calibration curve; (3) the existence of a minimum in the electrophoretic mobility-log $\kappa\underline{a}$ curve at certain values of the zeta potential and ionic strength. The variation of mobility with particle size described in the preceding sections demonstrates conclusively that the difference in migration distances is sufficient to determine the particle size of monodisperse polystyrene latexes. Indeed, the method is discriminating enough to separate samples with average diameters only 500 A. apart.

Figure 1 shows the theoretical variation of electrophoretic mobility with log $\kappa\underline{a}$ as a function of the zeta potential. The term $\kappa\underline{a}$ represents the ratio of the particle radius to the thickness of the double layer. For polystyrene latex particles in these media, the values of $\kappa\underline{a}$ are generally in the range 1-200. Over most of this range, the electrophoretic mobility increases with log $\kappa\underline{a}$, the increase being greater, the higher the zeta potential. The values of the zeta potential of polystyrene latex particles have not yet been definitively measured. After ion exchange, however, monodisperse polystyrene latexes prepared with persulfate initiator are stabilized only by chemically-bound sulfate endgroups of the polymer chains. The numbers of these endgroups have been determined, to give values of the surface charge density from which the zeta potential can be calculated, assuming that the surface charge density is equal to the surface potential ψ_0. Table VI shows that the values of the surface charge density for the polystyrene latexes used here fall in the range 1.6-8.3μC/cm^2, which corresponds to zeta potentials in the range 85-150 mv.

TABLE VI

Zeta Potentials of Polystyrene Latexes

Latex	Ave. Particle Diameter, A.	Surf. Chge. Density*, $\mu C/cm^2$	Zeta Potential**, mv	Microcapillary Zeta Potential***, mv
B	1090	2.1	98	---
D	1260	1.7	88	---
E	1760	1.7	86	---
F	2340	2.0	96	---
J	5000	2.1	98	---
L	7950	0	0	0
M	10400	5.8	150	25
O	13050	4.6	138	28
R	20200	3.8	130	25

*-determined by conductometric titration of ion-exchanged latex(18-21)
**-calculated from surface charge density for 2.5×10^{-3}M 1:1 electrolyte
***-determined in microcapillary cell in 2.5×10^{-3} M sodium barbital at 20°C

For zeta potentials of this magnitude, the electrophoretic mobilities should vary strongly with log κa. Moreover, in a mixture of monodisperse polystyrene latexes in a given medium, it may be assumed that the surface characteristics of the different sizes are similar, so that the variation of electrophoretic mobility with log κa is essentially the variation with log a. Therefore, under these conditions the electrophoretic mobility should be a measure of particle size. This is confirmed by Figures 6-8 which show mixtures of monodisperse polystyrene latexes separated into narrow streams.

Continuous particle electrophoresis does not yield absolute values of the electrophoretic mobility, but instead values of the relative migration distances under given conditions. This work shows that the migration distance varies in proportion to the voltage gradient and reciprocal electrolyte curtain flow rate, as predicted theoretically. Therefore, the values of the migration distance D may be normalized by multiplying by the electrolyte curtain flow rate F and the reciprocal voltage gradient 1/E, to give the factor DF/E. The value of this parameter is a measure of the relative electrophoretic mobility which allows the comparison of separations obtained at different electrolyte curtain flow rates, voltage gradients, and electrolyte concentrations (however, it should be emphasized that because of the electro-osmotic component in the displacement, DF/E generally is not equal to zero when the electrophoretic mobility is zero). Figure 9 shows the data of Figure 7 plotted as the variation of DF/E with log κa. The values of κ were calculated using the relationship applicable to a univalent electrolyte at 20° C.

$$\kappa = 3.27 \times 10^7 \, C^{\frac{1}{2}} \qquad (14)$$

where C is the concentration of electrolyte in moles/liter. It can be seen that the four sets of data of Figure 7 can be best fitted in Figure 9 by a single line, i. e., the incorporation of the factor κ reconciles the data.

Although the values of DF/E are only relative measures of the electrophoretic mobility, it is interesting to compare them with the theoretical relationships of Figure 1. All the experimental points of Figure 9 with the exception of those for Latex L are fitted well by the solid line that corresponds to the 26-mv curve of Figure 1 replotted on an arbitrary scale. Because the ordinate is scaled arbitrarily, the same points were compared with similarly replotted curves for higher values of the zeta potential. Although the fit for the 52-mv curve (not shown) was as good as that for the 26-mv curve, that for the 78-mv curve was poor, and those for higher values of the zeta potential became progressively worse. Thus, this comparison suggests that these monodisperse polystyrene latexes (with the exception of Latex L) have about the same value for the zeta potential --- in or near the 26-52 mv range --- and that the size separation depends upon

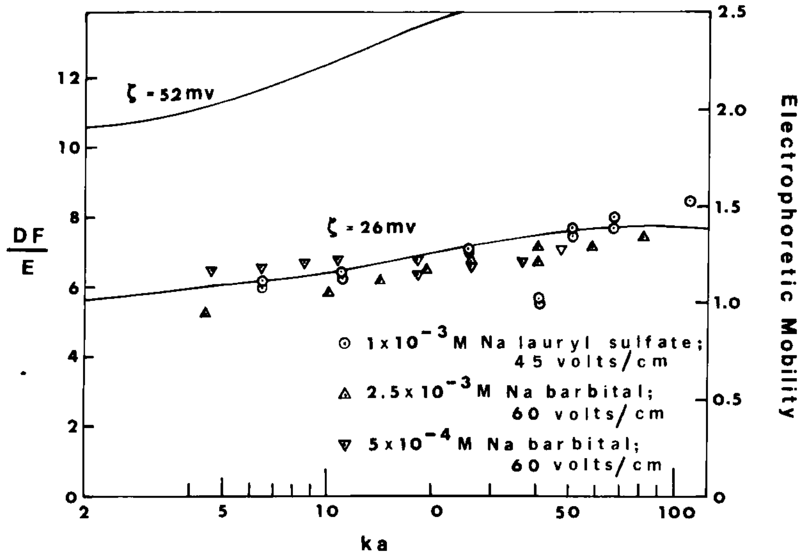

FIGURE 9

Variation of DF/E with Log Ka for Monodisperse Polystyrene Latexes.

the difference in the radius a. However, there are several arguments against this interpretation. First, implicit in this analysis is the assumption that the electro-osmotic component is zero, which is not the case; the value of this component has not been measured under these conditions, but it is almost certainly greater than zero and probably is significant compared to the values of DF/E. Second, although both curves for sodium barbital lie close together, that for the 2.5×10^{-3} M concentration has a slightly greater slope (i.e., a larger value of the zeta potential), while theoretical calculations for particles of constant surface charge show that the zeta potential increases with decreasing electrolyte concentration. Third, the zeta potential in 1×10^{-3} M sodium lauryl sulfate is expected to be greater than that in 5×10^{-4} M or 2.5×10^{-3} M sodium barbital because the equilibrium adsorption determined(22) for a similar monodisperse polystyrene latex was found to be 0.2×10^{-9} moles/cm^2 or 19μC/cm^2, which corresponds to an increase in the surface charge of 4-10 fold; however, the values of DF/E in sodium lauryl sulfate are not significantly different from those in sodium barbital. It is possible that these discrepancies can be explained by a dependence of the electro-osmotic component on the composition of the medium; however, until this parameter has been determined, no quantitative conclusions can be drawn about the zeta potentials derived in this way.

Four of the samples listed in Table VI are of microscopic size and therefore large enough to be measured by microcapillary electrophoresis. The values obtained for three of these latexes in 2.5×10^{-3} M sodium barbital lie in the range 25-28 mv, which confirms the correlation of the DF/E-log κa curve (Figure 9) with the line of Figure 1 corresponding to a zeta potential of 26 mv. The microcapillary electrophoresis measurements also explain why the migration distance of Latex L (the two points below the line of Figure 9) is considerably smaller than is usually observed for polystyrene particles of this size: the electrophoretic mobility and therefore the zeta potential is essentially zero. It would be tempting to use the migration distance of this latex as a calibration for the electro-osmotic component corresponding to zero charge; however, since this series of measurements was made in 1×10^{-3} M sodium lauryl sulfate, it is likely that some emulsifier adsorbed on the particle surfaces, increasing their surface charge somewhat but not up to the same level as that of the other polystyrene latexes. Moreover, when the migration distance of Latex L was taken as the electro-osmotic component at zero charge, a comparison of the recalculated DF/E-log κa curves with arbitrarily-replotted curves of Figure 1 showed that the slope of the experimental curve was much greater than that of any theoretical curve including that corresponding to a zeta potential of 156 mv, indicating that these particles bear at least a small change in this medium. Further characterization of Latex L using the method described earlier(23) showed that its particles are stabilized solely by surface hydroxyl endgroups of the polymer chains; these hydroxyl groups were determined by oxidation to the carboxyl form, followed by ion exchange and conductometric titration.

In order to correct the data of Figure 9 for the electro-osmotic component, the values of the migration distances for each series must be diminished by a constant amount (assuming the zeta potential of the cell walls to be constant). The proper electro-osmotic correction has not yet been determined; however, from the foregoing theoretical treatment, it is estimated to be equal to $D_r/3$. When the data of Figure 9 were recalculated using the migration distance observed for Latex L to determine the electro-osmotic correction and compared with the arbitrarily-replotted curves of Figure 1, the zeta potentials thus determined were in the range 78-104 mv (neither curve fitted the data well, but the fit for the 78-mv curve was slightly better than that for the 104-mv curve), values somewhat higher than those obtained assuming the electro-osmotic component to be zero. Similarly calculated values for other experiments given in Table VII show values of the zeta potential in the range 52-98 mv, also somewhat higher than those assuming zero electro-osmotic flow.

Another method of analyzing the data is to use the transit time of the particles in the cell to express the values of DF/E in absolute mobility units (μ sec^{-1} volt^{-1} cm). For example, for the data of Figures 7 and 9, an electrolyte curtain flow rate of 23.5 ml/min corresponds to a transit time in the field of $1180/F$ or about 50 sec. The values of the zeta potential thus determined are greater than the 156 mv value represented in the uppermost curve of Figure 1; however, this treatment also neglects the electro-osmotic component, so its results are probably greater than the actual values.

TABLE VII

Zeta Potentials of Polystyrene Latexes

Latex	Average Particle Diameter, A.	Sodium Barbital Concentration, M	Electrophoretic Mobility μ sec^{-1} volt^{-1} cm	Zeta Potential*, mv
C	1090	1×10^{-3}	2.0**	52
N	10990	1×10^{-3}	3.2**	64
C	1090	2.5×10^{-3}	2.4***	62
J	5000	2.5×10^{-3}	3.4***	67
C	1090	3.5×10^{-3}	2.5**	60
N	10990	3.5×10^{-3}	4.4**	80
C	1090	1×10^{-3}****	3.1***	~98
N	10990	1×10^{-3}****	4.4***	88

* - determined from Figure 1
** - corrected for electro-osmotic effect
*** - electro-osmotic correction -2.0 μ sec^{-1} volt^{-1} cm
**** - sodium lauryl sulfate instead of sodium barbital

The data were also analyzed using the apparent-degree-of-dissociation effect(19, 22), which was perceived when the concentration of H^+ ions in ion-exchanged monodisperse polystyrene latexes was measured in two different ways: (1) from the specific conductance of the latex; (2) from the endpoint of the conductometric titration with sodium hydroxide. Invariably, the two values do not agree: the number of H^+ ions determined by titration was greater than that number corresponding to the conductance of the latex. Thus, the latex behaves as if it contains fewer H^+ ions than are measured by direct titration. The ratio of the measured conductance to the conductance expected from the conductometric titration is defined as the apparent degree of dissociation α. Table VIII shows that the values of α found for various monodisperse polystyrene latexes(19, 22) are generally in the range 0.05-0.4 and decrease with increasing surface charge.

TABLE VIII

Zeta Potentials from Apparent Degree of Dissociation

Latex	Average Particle Diameter, A.	Surf. Chge. Density*, $\mu C/cm^2$	$\alpha^{(19, 22)}$	Diffuse Charge, $\mu C/cm^2$	Zeta Potential**, mv
D-1	1090	1.5	0.35	0.52	40
A-3 (F)	2340	2.0	0.39	0.78	55
A-2	880	3.3	0.21	0.69	50
B-1	1580	4.2	0.10	0.42	34
B-2 (G)	2480	5.7	0.054	0.31	26
D-4 (I)	4470	8.4	0.05	0.42	34

* - determined by conductometric titration of ion-exchanged latex(18-21)

** - calculated for 2.5×10^{-3} M 1:1 electrolyte

Thus, the strong-acid sulfate groups on the particle surface behave as if they were not completely dissociated, an unlikely possibility because of the strength of the acid group. A more likely explanation is that some H^+ ions are held very close to the particle surface (analogous to the theoretical Stern layer), while other H^+ ions are further away from the surface, in the diffuse double layer. Only those H^+ ions in the diffuse double layer contribute significantly to the conductance of the latex; those very close to the particle surface do not. The decrease in α with increasing surface charge density lessens the effect of the surface charge density on the electrophoretic mobility and probably is the reason for the good correlation of electrophoretic mobilities of latexes with similar surface characteristics but somewhat different surface charge densities (latexes with grossly-different surface charge densities do not show this correlation, e.g., the migration distances of Latex L which has zero surface charge falls well below the common curve of Figure 9). Moreover, the fact that α increases with increasing electrolyte concentration (not shown here) is consistent with the slight increase in migration distance with ionic strength.

The most important point of this analysis, however, is that the value of α can be used to estimate the zeta potential by assuming that the surface charge density determined by ion exchange and conductometric titration is equal to the surface potential ψ_0, that the division of H^+ ions between the Stern layer and the diffuse double layer is represented by the value of α, that this division occurs at a distance from the particle surface at which the potential is ζ, and that the value of α determined for the ion-exchanged latex (very low electrolyte concentration) is applicable to the same particles at a given electrolyte concentration, then combining these values with those from previously-calculated tables(28). Table VIII gives the values of the diffuse charge (the product of the surface charge density and α) and the corresponding zeta potentials in 2.5×10^{-3} M 1:1 electrolyte. These values are in the range 26-55 mv, in good agreement with the 26-52 mv range inferred by comparison of the curves of Figure 9 with the arbitratily-replotted curves of Figure 1. Moreover, the values of ζ / ψ_0 (not shown) are in the range 0.2-0.6, similar to the 0.3-0.5 range found for a wide variety of colloids under similar conditions(29).

This analysis can also be applied to the microscopic-size Latexes M, O, and R, which are measurable by microcapillary electrophoresis. Table IX gives the values of the surface charge density, α, and the diffuse charge, as well as a comparison of the experimental and calculated zeta potentials for various sodium barbital concentrations. For all three latexes, the values of ζ determined by microcapillary electrophoresis are in the range 25-28 mv for 2.5×10^{-3} M sodium barbital; with decreasing electrolyte concentration, these values increase to a maximum at 5.0×10^{-4} M, then fall off at 1.0×10^{-4} M. The reason for this maximum in the electrophoretic mobility-electrolyte concentration curve is not known; however, the increase with increasing electrolyte concentration in the range $1.0\text{-}5.0 \times 10^{-4}$ M is attributed speculatively to an increase in α. The exper-

TABLE IX

Zeta Potentials from Microcapillary Electrophoresis and Apparent Degree of Dissociation α

Latex	Average Particle Diameter, A.	Surf. Chge. Density*, $\mu C/cm^2$	α	Diffuse Charge, $\mu C/cm^2$	Zeta Potential, mv			
					(1)	(2)	(3)	(4)
		From Microcapillary Electrophoresis						
M	10400	5.8	0.15	0.87	25	35	76	66
O	13050	4.6	0.18	0.83	28	48	75	60
R	20200	3.8	0.29	1.10	25	40	95	76
		From Apparent Degree of Dissociation α						
M	10400	5.8	0.15	0.87	58	79	97	134
O	13050	4.6	0.18	0.83	56	77	94	133
R	20200	3.8	0.29	1.10	69	90	108	146

* - determined by conductometric titration of ion-exchanged latex

(1) 2.5×10^{-3} M sodium barbital

(2) 1.0×10^{-3} M sodium barbital

(3) 5.0×10^{-4} M sodium barbital

(4) 1.0×10^{-4} M sodium barbital

imental values are significantly smaller than those calculated from the values of α. Moreover, the calculated values increase monotonically with decreasing electrolyte concentration and show no maximum in this range of electrolyte concentration. The values of ζ/ψ_0 are in the range 0.4-0.7, again in agreement with those determined for other colloids(29).

The decrease in microcapillary electrophoretic mobility with increasing electrolyte concentration in the range $0.5\text{-}2.5 \times 10^{-3}$ M is in apparent disagreement with the increase in continuous-particle-electrophoresis migration distance in a similar range. However, the migration distances include the contribution of electro-osmotic flow, while the microcapillary electrophoresis measurements are made at the zero-solvent-flow level. An increase in electrophoretic mobility with increasing electrolyte concentration is not in accord with equation 2, but is to be expected from the more-complex relationship of Figure 1: if all particles of a colloid have the same surface charge density, the variation of electrophoretic mobility with log $\kappa \underline{a}$ is essentially the variation with log $\underline{a}$. Figure 1 shows an increase in electrophoretic mobility with log $\kappa \underline{a}$ in the range 5-1000; the higher the zeta potential, the sharper the increase. Therefore, an increase in electrolyte concentration should give an increase in electrophoretic mobility. Such an increase is not confirmed by measurements of the migration distances, however; Figure 7 shows that the values for the lower of two sodium barbital concentrations (0.5 and 2.5×10^{-3} M) are greater for particle sizes up to 2340 A., but the order is reversed at a particle size of 5000 A. Moreover, close examination of the normalized curves of Figure 9 shows that, although the points are fitted by a single curve, the values of $\underline{DF/E}$ decrease slightly with increasing electrolyte concentration for particle sizes up to 5000 A.; at larger particle sizes, the order may be reversed or at least is not well-defined. These results are consistent with the earlier data of Table IV, which shows that the migration distances at 2×10^{-3} M sodium barbital are significantly greater than at 1×10^{-3} M for a particle size of 2480 A., but the increase is not as well-demonstrated at particle sizes of 5000 A. and 10400 A.

On the other hand, the decrease in microcapillary electrophoretic mobility with increasing electrolyte concentration is demonstrated experimentally for particle sizes in the range 10400-20200 A., and this decrease is in agreement with the variation of calculated zeta potential based on the apparent degree of dissociation and the surface charge density. This comparison assumes that the "effective" (or diffuse) charge does not change with electrolyte concentration (i. e., the value of α determined for ion-exchanged latexes is applicable to the electrolyte concentrations used here).

However, the addition of electrolyte to these ion-exchanged latexes may increase the diffuse charge in two ways: (1) the electrolyte ions (in this case, diethyl barbiturate ions) may adsorb on the particle surface, thus increasing the surface charge density; (2) the value of α may increase, thus increasing the diffuse charge without altering the surface charge density. In addition, an increase in electrolyte concentration may alter the zeta potential of the cell walls and hence the electro-osmotic flow of the solvent. As will be shown below, however, there is no evidence for the adsorption of diethyl barbiturate ions on the latex particle surface. Moreover, although the values of α should increase with increasing electrolyte concentration, these values have not yet been measured for the monodisperse polystyrene latexes used here. Generally, an increase in the electrolyte concentration should cause a decrease in the electro-osmotic flow and hence a decrease in the migration distance; however, it is possible that the higher electrolyte concentration gives a greater decrease of the cell-wall zeta potential than that of the particles, leading to a net increase in the migration distance. In any event, the quantitative correlation of the continuous-particle-electrophoresis migration distances with the operating variables, experimental microcapillary electrophoretic mobilities, and the predictions of theory must await a more accurate determination of the necessary parameters.

The observed increase in migration distance with electrolyte concentration was at first attributed to adsorption of diethyl barbiturate ions from the buffer solution. This argument was supported by the fact that the migration distance was not affected significantly by the emulsifier concentration in the latex. The adsorption of a sufficient concentration of negative buffer ions would overshadow any difference in surface charge density arising from the presence or absence of adsorbed emulsifier, or a larger or smaller number of sulfate endgroups. To determine the possibility of such adsorption, a sample of ion-exchanged Latex J was diluted in deionized water and titrated conductometrically with 0.15 M sodium barbital. The conductance increased linearly with increasing concentration of sodium barbital and showed no discontinuity that might indicate the adsorption of diethyl barbiturate ions on the latex particle surface. Other experiments carried out by adding various concentrations of sodium barbital to ion-exchanged latexes, centrifuging the latexes to sediment the particles, and analyzing the supernatant layer by ultraviolet spectrophotometry also failed to give evidence for the adsorption of buffer ions.

The agreement within experimental error of the migration distances of the "as is," ion-exchanged, and ion-exchanged-plus-additional-emulsifier latexes may be explained by the equilibrium between adsorbed and solute emulsifier. In the "as is" (i. e., as prepared) latex, the equilibrium is such that most of the emulsifier is adsorbed on the particle surface and only a small proportion is dissolved in the aqueous phase. When the latex is diluted with water or electrolyte, however, emulsifier desorbs from the particle surface to maintain the equilibrium. When the latex sample is introduced into the electrolyte curtain, its aqueous serum is diluted many times, i. e., by the total volume of aqueous electrolyte in the cell. This extreme dilution leads to such drastic desorption of emulsifier that practically all of it is removed from the particle surface. Thus, the "as is" latexes display the same migration distance as the corresponding ion-exchanged latexes from which the emulsifier has been removed quantitatively, because the emulsifier is desorbed as effectively by extreme dilution as by ion exchange. Moreover, the addition of excess emulsifier to the ion-exchanged latex samples is not sufficient to prevent complete desorption upon dilution of the latex sample in the electrophoresis cell. Of course, in principle such desorption can be prevented by using aqueous anionic emulsifier (e.g., sodium lauryl sulfate) as the electrolyte.

In summary, continuous particle electrophoresis gives accurate and reproducible values for the relative electrophoretic mobilities of polystyrene latex particles, but the correlation needed to transform these relative values into absolute electrophoretic mobilities has not yet been developed.

CONCLUSIONS

The following conclusions can be drawn from this work: (1) continuous particle electrophoresis is a valuable tool for the separation of polystyrene latex particles according to size and for the determination of particle size and particle-size distribution within a few minutes; (2) from preliminary results with other latexes, it appears likely that this technique can be applied to the separation or particle-size determination of a wide variety of latexes and other colloidal sols; (3) this technique is particularly applicable to latexes of high zeta potential (however, it can also be applied to latexes of low zeta potential by adsorption of a highly-charged species to achieve a relatively-high and uniform zeta potential); (4) the separation of particles can be characterized not only by visual readings of the migration distance in mm, but also by measurements of the scattered-light intensity as a function of migration distance; (5) the migration distances measured at different voltage gradients, curtain electrolyte flow rates, and electrolyte concentrations when normalized can be fitted within experimental error by a single curve as a function of log $\kappa \underline{a}$; (6) absolute values for the electrophoretic mobility cannot yet be determined unequivocally because the electro-osmotic component for zero particle-charge is not known; (7) from the variation of migration distance with log $\kappa \underline{a}$, assuming the electro-osmotic component to be zero, the zeta potential of monodisperse polystyrene particles is estimated to be in the range 26-52 mv, as compared with the 86-150 mv range calculated assuming the measured surface charge density to be equal to the surface potential; (8) from the transit time in the electric field, also assuming the electro-osmotic component to be zero, the zeta potential is estimated to be in the range 50-90 mv; (9) the zeta potential estimated from the measured surface charge density and apparent degree of dissociation of bound surface groups is in the range 26-55 mv, in agreement with the measurements of microscopic-size particles by micro-capillary electrophoresis; (10) the quantitative correlation of the measured migration distances with absolute electrophoretic mobilities must await the more accurate determination of the electro-osmotic component of the electrophoresis cell as well as the surface characteristics of the latex particles.

ACKNOWLEDGMENTS

The authors acknowledge gratefully the contributions of E. B. Bradford for the particle-size measurements by electron microscopy, J. B. Shaffer for the preparation of some of the latex samples, and Dr. H. J. van den Hul for some measurements of surface charge density and for many helpful suggestions for analysis of the data.

REFERENCES

1. Present address, Center for Surface and Coatings Research, Lehigh University, Bethlehem, Pa. 18015.
2. J. Th. G. Overbeek & H. G. Bungenberg de Jong, "Colloid Science Vol. II. Reversible Systems," H. R. Kruyt, editor, Elsevier, Amsterdam-New York, 1949, p. 194.
3. M. von Smoluchowski, Z. physik. Chem. 92, 129 (1917); J. Chem. Soc. 112, II, 297 (1917).
4. E. Hückel, Physik Z. 25, 204 (1924).
5. D. C. Henry, Proc. Soc. London A133, 106 (1931).
6. J. Th. G. Overbeek, thesis, University of Utrecht, 1941.
7. J. Th. G. Overbeek, Kolloidchem. Beihefte 54, 287 (1943).

8. F. Booth, Nature 161, 83 (1948).

9. F. Booth, Proc. Roy. Soc. London A203, 514 (1950).

10. P. H. Wiersema, thesis, University of Utrecht, 1964.

11. P. H. Wiersema, A. L. Loeb, & J. Th. G. Overbeek, J. Colloid & Interface Sci. 22, 78 (1966).

12. K. Hannig, Z. Anal. Chem. 181, 244 (1961).

13. K. Hannig, Hoppe-Seyler's A. Physiol. Chem. 338, 211 (1964).

14. A. Strickler, A. Kaplan, & E. Vigh, Microchem. J. 10, 529 (1966).

15. A. Strickler, Separation Sci. 2, 335 (1967).

16. J. W. Vanderhoff, J. F. Vitkuske, E. B. Bradford, & T. Alfrey, Jr., J. Polymer Sci. 20, 225 (1956).

17. E. B. Bradford & J. W. Vanderhoff, J. Appl. Phys. 26, 864 (1955).

18. H. J. van den Hul & J. W. Vanderhoff, J. Colloid & Interface Sci. 28, 336 (1968).

19. J. W. Vanderhoff, H. J. van den Hul, R. J. M. Tausk, & J. Th. G. Overbeek, "Clean Surfaces: Their Preparation and Characterization for Interfacial Studies," G. Goldfinger, editor, Marcel Dekker, New York, 1970, p. 15.

20. G. D. McCann, E. B. Bradford, H. J. van den Hul, & J. W. Vanderhoff, "Polymer Colloids," R. M. Fitch, editor, Plenum Press, New York, 1971, p. 29.

21. H. J. van den Hul & J. W. Vanderhoff, J. Electroanal. & Interfacial Electrochem. 37, 161 (1972).

22. H. J. van den Hul & J. W. Vanderhoff, "Polymer Colloids," R. M. Fitch, editor, Plenum Press, New York, 1971, p. 1.

23. H. J. van den Hul & J. W. Vanderhoff, Brit. Polymer J. 2, 121, (1970).

24. M. von Smoluchowski, Bull. acad. Sci. Cracovic 182 (1903).

25. I. Johnson & V. K. LaMer, J. Am. Chem. Soc. 69, 1184 (1947).

26. V. K. LaMer & I. W. Plesner, J. Polymer Sci. 24, 147 (1957).

27. M. Kerker, E. Daby, G. L. Cohen, J. P. Kratohvil, & E. Matijevic, J. Phys. Chem. 67, 2105 (1963).

28. A. L. Loeb, J. Th. G. Overbeek & P. H. Wiersema, "The Electrical Double Layer Around a Spherical Colloidal Particle," the M. I. T. Press, Cambridge, Massachusetts, 1961.

29. J. T. Davies & E. K. Rideal, "Interfacial Phenomena," Academic Press, London, 1963, p. 140-46.